ISSN 3047-5473
Innovation in Engineering, Vol. 3, No. 1, 2026, pp. 11-23

Design, CFD analysis, and experimental validation of a NACA 4415 ducted hydrokinetic turbine for low-velocity river applications

Ma. Leona Maye B. Pepito*, Kent B. Ignali, Ian Keanu E. Becoy, Keith John D. Tadifa and John Kenno P. Lumasag

College of Engineering and Architecture, University of Science and Technology of Southern Philippines, **Philippines**

*Corresponding Author: leona.pepito@ustp.edu.ph

Received: 14 December 2025; *Revised*: 12 February 2026; *Accepted*: 22 February 2026

DOI: https://doi.org/10.58712/ie.v3i1.43

Abstract: Hydrokinetic turbines represent a promising solution for renewable energy generation in low-velocity rivers where conventional hydropower systems are not technically or economically feasible. Despite increasing interest in ducted hydrokinetic turbines, experimental validation of turbines employing the NACA 4415 airfoil under low-flow river conditions remains limited. This study presents the design, computational fluid dynamics (CFD) analysis, and experimental validation of a horizontal-axis ducted hydrokinetic turbine using the NACA 4415 airfoil, specifically optimized for low-velocity river applications. Numerical simulations and field experiments were conducted for water velocities ranging from 0.89 to 1.03 m/s to evaluate turbine performance in terms of rotational speed, torque, power output, and power coefficient. The results indicate that the four-bladed ducted turbine achieved a maximum experimental power output of 67 W at a flow velocity of 1.03 m/s, corresponding to a power coefficient of 0.32. The diffuser-augmented configuration enhanced flow acceleration and rotational speed compared to theoretical predictions and numerical simulations, although performance discrepancies were observed due to hydrodynamic losses and mechanical inefficiencies. Overall, the findings demonstrate the feasibility and effectiveness of NACA 4415 ducted hydrokinetic turbines for decentralized renewable energy generation in low-flow river environments, contributing valuable experimental data for the development and optimization of small-scale hydrokinetic systems.

Keywords: energy sufficiency and security; hydrokinetic turbine; renewable energy; diffuser-augmented; clean energy

1. Introduction

Renewable energy sources play a vital role in addressing global challenges related to climate change, environmental degradation, and the continuously increasing demand for energy [1], [2]. Conventional fossil fuel-based energy systems contribute significantly to greenhouse gas emissions and are subject to long-term resource depletion, thereby accelerating the global transition toward sustainable and low-carbon energy alternatives [3]. Among various renewable energy options, hydropower remains one of the most mature and widely deployed technologies, contributing a substantial share to global electricity generation [4]. However, conventional hydropower systems are highly dependent on sufficient hydraulic head and extensive infrastructure, which limits their feasibility in low-head and shallow river environments commonly found in rural and remote regions.

Recent developments in hydropower technology have increasingly focused on hydrokinetic energy (HKE), which harnesses the kinetic energy of flowing water without the need for dams or major civil

works [5]. Hydrokinetic turbines directly convert the kinetic energy of river or canal flows into mechanical power and subsequently into electricity through generators and power electronics. Owing to their minimal infrastructure requirements, these systems are particularly suitable for decentralized power generation in low-speed and shallow water environments. Nevertheless, the performance of hydrokinetic turbines is strongly constrained by low flow velocities, which are typically below 1.5 m/s in small rivers. Under such conditions, conventional turbine designs often suffer from low power output and reduced efficiency, posing a significant technical challenge for practical implementation [6].

The hydrodynamic performance of hydrokinetic turbines is strongly influenced by blade design parameters, including airfoil profile, number of blades, and operating Reynolds number. Among various airfoil profiles, the NACA 4415 airfoil has been identified as a promising candidate for hydrokinetic applications due to its favorable lift-to-drag characteristics under low-speed flow conditions [7]. Previous studies have reported that turbines employing the NACA 4415 profile can achieve higher power coefficients than those using symmetrical airfoils, particularly in low-velocity water currents [8]. Despite these promising findings, most existing studies rely primarily on numerical simulations or laboratory-scale experiments, with limited validation under real river flow conditions.

In addition to blade optimization, the implementation of ducted or diffuser-augmented configurations has been proposed as an effective strategy to enhance hydrokinetic turbine performance [9], [10], [11], [12]. The incorporation of a duct and diffuser can accelerate the incoming flow by inducing a pressure drop at the turbine exit, thereby increasing the effective mass flow rate through the rotor and improving overall energy extraction efficiency [13]. Although previous studies have demonstrated the potential benefits of diffuser-augmented turbines, their performance is highly sensitive to geometric parameters such as duct length, diffuser angle, and rotor placement. Furthermore, experimental investigations that systematically evaluate ducted hydrokinetic turbines operating in low-velocity natural water bodies remain scarce.

Despite the growing interest in hydrokinetic turbine technologies, a clear research gap persists in the combined numerical and experimental assessment of NACA 4415-based ducted hydrokinetic turbines under low-flow river conditions. In particular, there is a lack of field-scale experimental data that validate computational fluid dynamics (CFD) predictions and quantify real-world performance losses associated with hydrodynamic effects and mechanical inefficiencies. Therefore, this study aims to design, simulate, and experimentally validate a horizontal-axis ducted hydrokinetic turbine employing the NACA 4415 airfoil, specifically optimized for low-velocity river applications. The novelty of this work lies in the integration of CFD analysis with experimental performance evaluation in a natural river environment, providing practical insights into the feasibility and performance of small-scale ducted hydrokinetic turbines for decentralized renewable energy generation.

2. Material and methods

2.1 Site characteristics and flow measurements

The hydrokinetic turbine was designed and evaluated based on the characteristics of a natural river site located at Bobonawan River, Sitio Kalasuyan, Barangay Capihan, Libona, Bukidnon, Philippines (8°14′31″ N, 124°46′06″ E). Site characterization was conducted to obtain representative flow conditions for turbine design and performance assessment. Water velocity measurements were performed using the float method, which is commonly applied for preliminary flow assessment in shallow rivers. A lightweight floating object was released along a measured distance, and the travel time was recorded to estimate the surface flow velocity. Multiple measurements were conducted to minimize random error, and the resulting flow velocities ranged from 0.89 m/s to 1.03 m/s, representing low-velocity river conditions suitable for hydrokinetic applications.

Figure 1. Bobonawan river

The theoretical power available in the flowing water was estimated using the classical kinetic energy Equation (1).

$$P = \frac{1}{2}\rho A V^3 \quad (1)$$

where $P$is the available power (W), $\rho$is the water density (kg/m³), A is the cross-sectional area (m²), and V is the water velocity (m/s). This equation provides a baseline estimate of the maximum kinetic energy available for conversion and serves as a reference for evaluating turbine performance under different flow velocities.

The actual mechanical power extracted by the turbine shaft is expressed as Equation (2).

$$P_{out} = \frac{1}{2}\rho\, A\, V^3 C_p C_n \quad (2)$$

where P_{out} is the shaft power output (W), C_p is the power coefficient representing the hydrodynamic efficiency of the turbine, and C_n is the mechanical efficiency accounting for drivetrain and generator losses. The power coefficient is calculated using Equation (3).

$$C_p = \frac{P_{out}}{\left(\frac{1}{2}\rho\, A\, V^3\right)} \quad (3)$$

which represents the fraction of the available kinetic power converted into useful mechanical power by the turbine. The operating condition of the turbine is characterized by the tip speed ratio (TSR), defined as Equation (4).

$$\lambda = \omega \frac{R}{V} \quad (4)$$

where λ is the tip speed ratio, ω is the angular velocity of the rotor (rad/s), R is the rotor radius (m), and V is the flow velocity (m/s).

2.2 Turbine design configuration

The design of the ducted hydrokinetic turbine model is presented in Figure 2. A horizontal-axis hydrokinetic turbine employing the NACA 4415 airfoil was designed for low-velocity river operation. The rotor consists of four blades, selected based on prior studies indicating improved performance and mechanical stability for multi-bladed turbines operating at low tip-speed ratios. The blade geometry was generated using NACA 4415 airfoil coordinates and discretized into ten spanwise sections. Each section was defined by its chord length, twist angle, and relative flow angle to ensure optimal

interaction with the incoming water flow. The blade geometry was modeled in SolidWorks for both numerical simulation and fabrication.

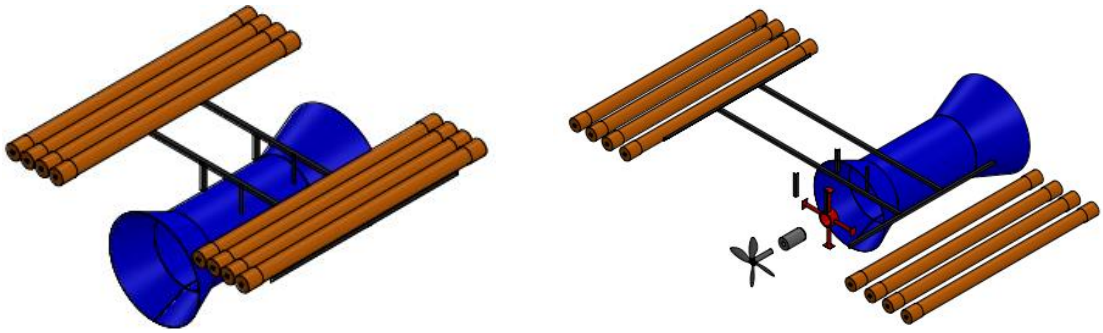

Figure 2. Ducted hydrokinetic turbine

2.2.1 Blade design

The different number of blades affects the performance of ducted hydrokinetic turbine in terms of performance and its overall efficiency. With specific number of blades based on various factors such as the speed and volume of the flowing water, the desired rotational speed of the turbine, and the desired power output. The NACA 4415, power coefficient was improved 26% for 0.5 – 2 m/s and 50% for speed of 2 – 3 m/s stream velocities [7]. NACA 4415 is suitable in low stream velocity that draws more energy generation for low stream rivers [8]. NACA 4415 is known for its stability in both low and high-speed water currents. This stability allows the turbine to operate in varying conditions. These ensure that the turbine can effectively harness energy from water currents in a wide range of flow conditions, making the NACA 4415 ideal for reliable and efficient power generation in hydrokinetic. The available power of flowing water is calculated using Equation (5).

$$P = \frac{1}{2}\rho A V^3 C_p C_n \quad (5)$$

where (P) denotes the available power (W), (ρ) is the water density (kg/m^3), (A) represents the cross-sectional area of the flow (m^2), (V) is the flow velocity (m/s), Cp is the power coefficient and Cn is the mechanical efficiency.

These blades are designed to interact efficiently with water currents, in a manner analogous to wind turbine blades operating in air. They are typically curved or airfoil-shaped to maximize energy capture while minimizing hydrodynamic drag. As water flows over the blades, lift and drag forces are generated, causing the turbine rotor to rotate and thereby converting the kinetic energy of the flowing water into rotational mechanical energy. The airfoil coordinates were prepared and input into Microsoft Excel to enable accurate geometric plotting in SolidWorks. The blade geometry was discretized into ten spanwise sections, each defined by a specific plane number with a corresponding plane spacing, relative velocity (ϕ), blade twist angle (β), and chord length (c). The tip speed ratio was determined based on the results obtained from the SolidWorks simulation.

Table 1. NACA 4415 properties

Parameter	NACA 4415
Blade pitch angle	7^0
Lift coefficient	3. 961
Drag coefficient	0.2

The NACA 4415 propeller blade for the hydrokinetic turbine is constructed using fiberglass reinforced with non-sag epoxy, combining durability, flexibility, and lightweight properties. This material choice provides a high strength-to-weight ratio, essential for efficient energy capture in water flow conditions, while also offering superior resistance to fatigue and corrosion. These characteristics make it a reliable option for long-term use in aquatic environments, ensuring performance under varying flow velocities. The blade's design and material enhance energy transfer efficiency, making it ideal for hydrokinetic applications.

Figure 3. Fabricated NACA 4415

2.2.2 Diffuser design

A diffuser illustrated in Figure 4, is typically used to increase the flow velocity that enters the turbine, resulting in a higher power rate and increasing the efficiency of the system. The area ratio ranges from 1.2 to 2, and the diffuser angle ranges from 5 degrees to 15 degrees. Also, adding a shroud at length to rotor diameter ratio of 0.5 and the clearance from blade to cover should have a distance of 3% of the rotor blade can increase the performance efficiency because of the more concentrated fluid flow.

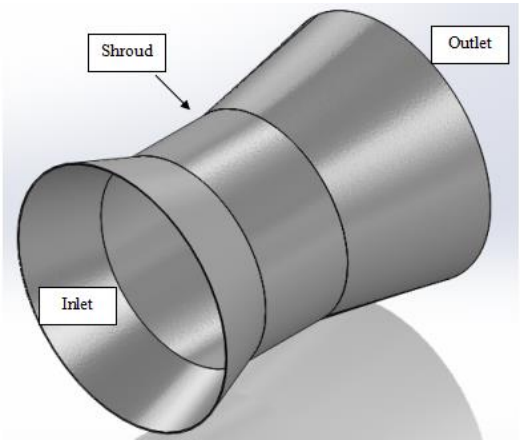

Figure 4. Venturi Duct diffuser housing design

The venturi duct dimensions are summarized in Table 2 where the fluid pressure decreases as the fluid passes through the constricted section where the turbine blade is located, thus allowing more fluid to pass through at high velocity.

Table 2. Dimensions of the venturi duct housing

Parameters	Dimensions
Area Ratio of Diffuser	1.6
Diffuser angle inlet	18 degrees
Diffuser angle outlet	9 degrees
Diameter of shroud	0.497 m
Diameter of diffuser	0.628 m (inlet and outlet)
Length of Shroud	0.249m
Total Length of the Housing	0.8 m

2.2.3 Nacelle design

The nacelle consists of three modular components: head, body, and tail. As shown in Figure 5, the assembly utilizes threaded connections with integrated rubber O-rings to ensure watertight sealing under submerged operating conditions. The modular configuration allows the head and tail sections to be detached independently from the main body for maintenance and inspection. The nacelle housing is fabricated from engineering-grade polymer to provide corrosion resistance, dimensional stability, and reduced weight. The head section accommodates the bearing housing and shaft support system, enabling bearing replacement or servicing without disassembling the entire nacelle–diffuser assembly. This modular design enhances maintainability while preserving structural integrity and hydrodynamic alignment.

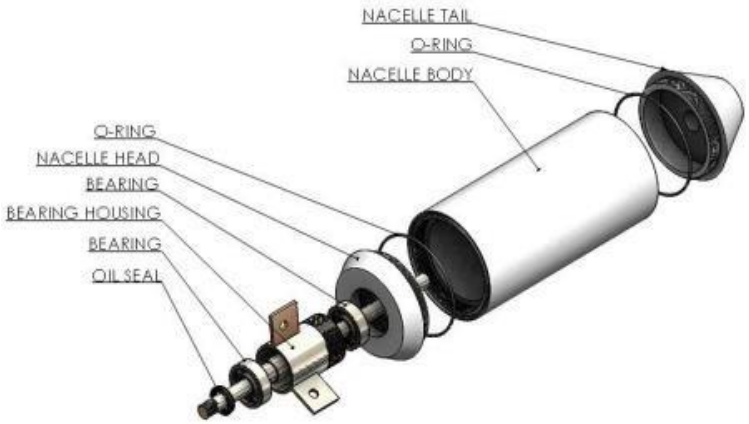

Figure 5. Nacelle assembly exploded view

2.3 CFD simulation

Computational fluid dynamics (CFD) simulations were performed using the Flow Simulation module in SolidWorks Perpetual License 2022 to analyze the hydrodynamic performance of the ducted hydrokinetic turbine. The simulations were conducted under steady-state, incompressible flow conditions, assuming water as a Newtonian fluid with constant properties at standard temperature. The governing equations solved include the three-dimensional Reynolds-averaged Navier–Stokes (RANS) equations for mass and momentum conservation. Turbulence effects were modeled using the realizable k–ε turbulence model, which provides a reasonable balance between computational efficiency and accuracy for internal and external flow problems involving moderate turbulence intensity and flow separation. This model has been widely applied in hydrokinetic and ducted turbine simulations due to its robustness in predicting flow behavior in confined geometries.

The computational domain encompassed the complete turbine assembly, including the rotor, duct, cylindrical section, and diffuser. A uniform velocity inlet boundary condition was applied at the upstream domain corresponding to measured river flow velocities ranging from 0.89 m/s to 1.03 m/s. A pressure outlet boundary condition was specified at the downstream boundary, while no-slip wall conditions were applied to all solid surfaces. The rotor motion was modeled using a rotating reference frame approach, enabling the prediction of torque and rotational effects without transient blade-resolved simulation.

A hybrid mesh consisting of tetrahedral elements with localized mesh refinement near the blade surfaces, duct walls, and diffuser region was generated. Mesh refinement was applied to ensure adequate resolution of boundary layers and regions with high velocity gradients. A mesh independence study was conducted by progressively increasing the mesh density until variations in predicted torque and power output were below 5%, ensuring numerical accuracy while maintaining computational efficiency. Key performance parameters, including torque, rotational speed, shaft power, and power coefficient, were extracted from the CFD simulations. These numerical results were subsequently compared with theoretical predictions and experimental measurements to validate the simulation framework and assess the effectiveness of the ducted turbine configuration under low-velocity flow conditions.

2.4 Fabrication and experimental setup

The hydrokinetic turbine prototype was fabricated based on the finalized design parameters. The turbine blades were constructed using fiberglass reinforced with epoxy resin to achieve a high strength-to-weight ratio and corrosion resistance suitable for aquatic environments. The duct, cylinder, and diffuser components were fabricated from aluminum due to its lightweight characteristics, durability, and resistance to corrosion. The assembled turbine system was deployed at the selected river site and tested under natural flow conditions. Rotational speed, torque, and electrical power output were measured during operation to evaluate actual turbine performance.

(a) (b) (c)

Figure 6. Fabrication process of ducted hydrokinetic turbine. (a) Assembling of parts (b) Final welding (c) Final adjustment of hydrokinetic ducted design

2.5 Performance evaluation

The experimental performance of the turbine was evaluated by comparing measured power output, rotational speed, and torque against theoretical predictions and CFD simulation results. The power coefficient (C_p) was calculated to quantify the efficiency of kinetic energy conversion under varying flow velocities. This comparative analysis enabled assessment of the effectiveness of the ducted configuration and identification of performance discrepancies arising from hydrodynamic losses and mechanical inefficiencies.

2.6 Uncertainty and measurement error analysis

An uncertainty analysis was performed to assess the reliability of experimental measurements and their impact on calculated performance parameters. The uncertainty in flow velocity measurements using the float method was estimated at ±8%, primarily due to surface flow effects and timing inaccuracies. Rotational speed measurements exhibited an uncertainty of ±5%, while torque measurements showed an uncertainty of ±7% due to sensor resolution and mechanical losses. The combined uncertainty in power output was calculated using standard error propagation methods, resulting in an estimated overall uncertainty of approximately ±10%. This uncertainty range was considered when comparing experimental results with CFD predictions and theoretical estimates.

3. Results and discussion

3.1 CFD simulation results and blade configuration analysis

Figure 7 presents the CFD simulation model of the ducted hydrokinetic turbine used to evaluate the influence of blade number on turbine performance under low-velocity flow conditions. Simulations were conducted for blade configurations ranging from three to seven blades at a representative flow velocity of 1.03 m/s, corresponding to the upper range of the measured river velocity. The performance indicators extracted from the simulations include torque, rotational speed, shaft power, and tip speed ratio (TSR, λ).

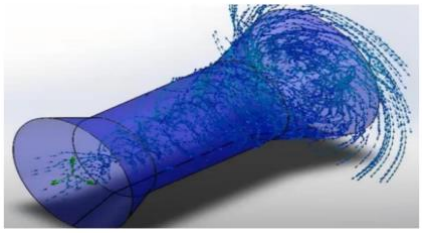

Figure 7. Simulation model of ducted hydrokinetic turbine

The numerical results indicate that the four-bladed configuration provides an optimal balance between torque generation and rotational speed. Configurations with fewer blades exhibited higher rotational speeds but insufficient torque, while configurations with more than four blades resulted in increased flow blockage and viscous losses, leading to reduced efficiency. The optimal CFD-predicted TSR for the four-bladed turbine was approximately $\lambda \approx 3.2$, which is consistent with the theoretical design TSR for low-speed hydrokinetic turbines reported in the literature. This TSR value was therefore adopted as the design reference for experimental validation.

3.2 Comparison of theoretical, CFD and experimental results

Figure 8 compares theoretical predictions, CFD simulation results, and experimental measurements for rotational speed, torque, and power output at flow velocities of 0.89 m/s and 1.03 m/s. At a flow velocity of 0.89 m/s, the theoretical model predicts a power output of 58.57 W, with a rotational speed of 104 rpm and torque of 5.38 Nm. The CFD simulation yields a lower power output of 42.75 W at 67 rpm, reflecting viscous and turbulence-related losses captured by the numerical model. Experimental measurements indicate a power output of 46 W, with a significantly higher rotational speed of 270 rpm and a lower torque of 2.2 Nm.

At the higher flow velocity of 1.03 m/s, the theoretical power output increases to 91 W with a predicted rotational speed of 120 rpm and torque of 7.23 Nm. The CFD results indicate a power

output of 62.71 W at 71 rpm and torque of 8.42 Nm, while experimental testing records a maximum power output of 67 W at 300 rpm and torque of 2.8 Nm. The closer agreement between CFD and experimental power outputs at this velocity, with a relative deviation of approximately 7%, demonstrates the validity of the CFD framework in predicting overall turbine performance under low-flow conditions.

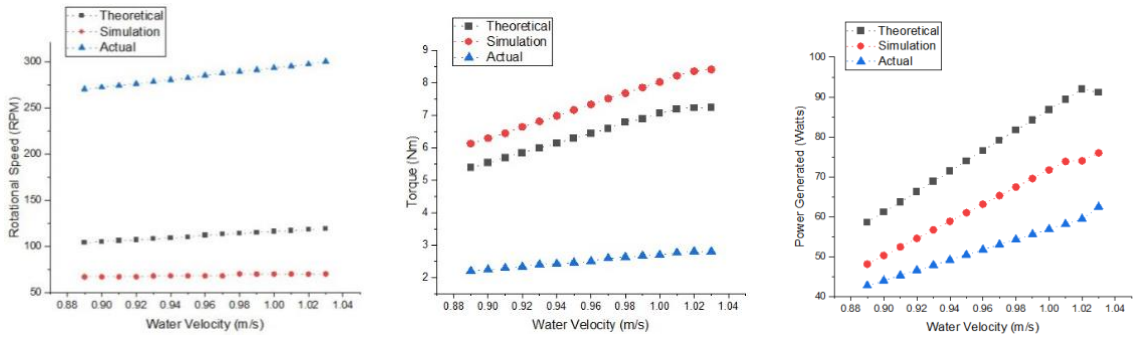

(a) (b) (c)

Figure 8. Comparison of theoretical, simulated and actual results. (a) Rotational speed, (b) Torque, (c) Power generated with the varying stream velocity

The discrepancies observed between theoretical, numerical, and experimental rotational speeds are primarily attributed to mechanical losses, drivetrain friction, flow non-uniformity, and limitations of the steady-state CFD approach. While the CFD model captures hydrodynamic behavior within the ducted turbine, it does not fully account for bearing losses, generator loading effects, and transient flow fluctuations present during field operation.

3.3 Power coefficient and tip speed ratio analysis

Figure 9 illustrates the variation of shaft power and power coefficient (Cp) as a function of flow velocity. Both CFD and experimental results exhibit similar increasing trends with increasing water velocity, confirming the expected cubic relationship between flow velocity and extractable power. At the minimum flow velocity of 0.89 m/s, the experimentally obtained power coefficient is approximately Cp = 0.23, while at the maximum flow velocity of 1.03 m/s, Cp increases to approximately 0.32. This validates the optimum Cp as a function of design TSR (g=3.2) for a 4-bladed turbine [13].

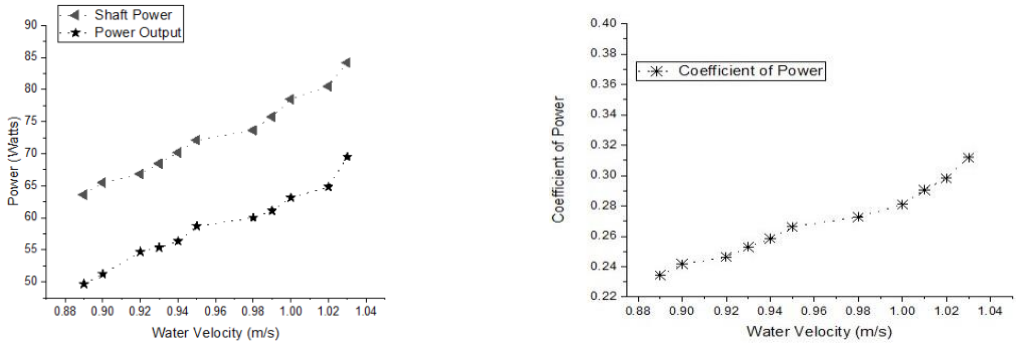

(a) (b)

Figure 9. (a) Shaft power and power output, and (b) Coefficient of tower

The experimentally observed Cp values correspond to an operational TSR range of $\lambda \approx 3.0–3.3$, which is consistent with the CFD-predicted optimal TSR of $\lambda \approx 3.2$ for the four-bladed turbine configuration. This agreement confirms that the turbine operated close to its designed hydrodynamic condition during field testing. Minor deviations between CFD-predicted and experimentally measured Cp values can be attributed to uncertainties in flow velocity measurement (±8%), torque measurement (±7%), and rotational speed measurement (±5%), as discussed in the uncertainty analysis section. The inclusion of uncertainty analysis provides essential context for interpreting the observed discrepancies between theoretical, numerical, and experimental results. The combined experimental uncertainty in power output was estimated at approximately ±10%, which adequately explains the differences observed between CFD-predicted and measured power values. Notably, the CFD predictions fall within the experimental uncertainty bounds for both flow velocities, supporting the reliability of the numerical model for performance estimation.

Although the CFD simulations were conducted under steady-state conditions using a rotating reference frame, the model successfully captured the dominant hydrodynamic trends and performance characteristics of the ducted hydrokinetic turbine. Future improvements could include transient simulations and detailed blade-resolved modeling to further reduce discrepancies and capture unsteady flow effects. Nevertheless, the current CFD framework provides a computationally efficient and sufficiently accurate tool for preliminary design and optimization of ducted hydrokinetic turbines operating in low-velocity river environments [14], [15], [16]. Overall, the combined CFD and experimental results demonstrate that the four-bladed NACA 4415 ducted hydrokinetic turbine performs effectively under low-flow river conditions. The close agreement between CFD predictions and experimental measurements, when uncertainty is considered, validates the numerical approach and confirms the suitability of the selected blade profile, duct configuration, and design TSR. These findings highlight the potential of diffuser-augmented hydrokinetic turbines for decentralized renewable energy generation in low-velocity natural water bodies.

4. Conclusion

This study presented the design, numerical simulation, and experimental validation of a horizontal-axis ducted hydrokinetic turbine employing the NACA 4415 airfoil for low-velocity river applications. The turbine was specifically optimized to operate under flow velocities ranging from 0.89 m/s to 1.03 m/s, which are commonly encountered in shallow and low-head rivers. By integrating blade profile optimization with a diffuser-augmented configuration, the proposed turbine demonstrates improved energy extraction capability under constrained flow conditions. Computational fluid dynamics (CFD) simulations were conducted to evaluate turbine hydrodynamic performance and to identify the optimal blade configuration and operating conditions. The four-bladed rotor configuration was found to provide the most favorable balance between torque generation and rotational speed, operating at an optimal tip speed ratio of approximately $\lambda \approx 3.2$. The CFD predictions of torque, power output, and power coefficient exhibited good agreement with experimental measurements when experimental uncertainties were taken into account, confirming the reliability of the numerical framework for performance estimation.Experimental testing under natural river flow conditions demonstrated that the ducted hydrokinetic turbine achieved a maximum power output of 67 W at a flow velocity of 1.03 m/s, with corresponding power coefficient values increasing from approximately $Cp = 0.23$ at 0.89 m/s to $Cp = 0.32$ at 1.03 m/s. The experimentally observed operational TSR range of $\lambda \approx 3.0–3.3$ closely matched the CFD-predicted optimal TSR, indicating that the turbine operated near its designed hydrodynamic condition during field deployment. The discrepancies observed between theoretical predictions, CFD results, and experimental measurements were primarily attributed to hydrodynamic losses, mechanical inefficiencies, and flow measurement uncertainties inherent to field testing. An uncertainty analysis indicated an overall experimental power uncertainty of approximately ±10%,

within which the CFD predictions consistently fell. This validation confirms that the combined CFD–experimental approach adopted in this study is suitable for the preliminary design and evaluation of small-scale ducted hydrokinetic turbines operating in low-velocity river environments. The findings of this study highlight the feasibility and effectiveness of NACA 4415-based ducted hydrokinetic turbines for decentralized renewable energy generation in low-flow natural water bodies. Future work should focus on transient CFD simulations, long-term field testing, and optimization of duct geometry and generator coupling to further enhance performance and reliability under variable flow conditions

Author's declaration

Author contribution

Ma. Leona Maye B. Pepito: Conceptualization, supervision and validation. **Kent B. Ignalig**: Investigation, methodology and resources. **Ian Keanu E. Becoy**: Formal analysis, methodology and resources. **Keith John D. Tadifa**: Investigation, methodology and resources. **John Kenno P. Lumasag**: Project administration, methodology and resources.

Funding statement

This research received no specific grant from any funding agency in the public, commercial, or not-for-profit sectors.

Data availability

The data that support the findings of this study are available from the corresponding author upon reasonable request. The data include CFD simulation outputs, experimental measurements, and processed performance results used in the analysis.

Acknowledgements

The authors would like to acknowledge the support of the University of Science and Technology of Southern Philippines for providing facilities and technical assistance necessary for the completion of this study. The authors also extend their appreciation to the local community of Barangay Capihan, Libona, Bukidnon, for permitting access to the river site during experimental testing.

Conflict of interest

The authors declare that they have no known competing financial interests or personal relationships that could have appeared to influence the work reported in this paper.

Ethical clearance

This study did not involve human participants, animals, or sensitive personal data. Therefore, ethical approval was not required.

AI statements

Artificial intelligence tools were not used in the design, data collection, analysis, or interpretation of results for this study. AI-assisted tools were used only for language editing and grammar refinement, without affecting the scientific content or conclusions of the manuscript.

Publisher's and Journal's Note

Researcher and Lecturer Society as the publisher, and the Editor of Innovation in Engineering state that there is no conflict of interest towards this article publication.

References

[1] A. Sompolska-Rzechuła, I. Bąk, A. Becker, H. Marjak, and J. Perzyńska, "The Use of Renewable Energy Sources and Environmental Degradation in EU Countries," *Sustainability*, vol. 16, no. 23, p. 10416, Nov. 2024, https://doi.org/10.3390/su162310416

[2] M. M. Naseer, A. I. Hunjra, A. Palma, and T. Bagh, "Sustainable development goals and environmental performance: Exploring the contribution of governance, energy, and growth," *Res. Int. Bus. Finance*, vol. 73, p. 102646, Jan. 2025, https://doi.org/10.1016/J.RIBAF.2024.102646

[3] J. Wang and W. Azam, "Natural resource scarcity, fossil fuel energy consumption, and total greenhouse gas emissions in top emitting countries," *Geoscience Frontiers*, vol. 15, no. 2, p. 101757, Mar. 2024, https://doi.org/10.1016/J.GSF.2023.101757

[4] M. Asif, *Handbook of Energy Transitions*. Boca Raton: CRC Press, 2022. https://doi.org/10.1201/9781003315353

[5] W. I. Ibrahim, M. R. Mohamed, R. M. T. R. Ismail, P. K. Leung, W. W. Xing, and A. A. Shah, "Hydrokinetic energy harnessing technologies: A review," *Energy Reports*, vol. 7, pp. 2021–2042, Nov. 2021, https://doi.org/10.1016/J.EGYR.2021.04.003

[6] P. B. Ngancha, B. P. Numbi, and K. Kusakana, "Optimal potential of cascading the hydro-power energy generation site, with a hydrokinetic turbine generation system. A case study analysis in the Southern African region," *Heliyon*, vol. 10, no. 20, p. e39663, Oct. 2024, https://doi.org/10.1016/J.HELIYON.2024.E39663

[7] S. Mohammadi, M. Hassanalian, H. Arionfard, and S. Bakhtiyarov, "Optimal design of hydrokinetic turbine for low-speed water flow in Golden Gate Strait," *Renew. Energy*, vol. 150, pp. 147–155, May 2020, https://doi.org/10.1016/J.RENENE.2019.12.142

[8] B. S. Jasim, A. A. Shandookh, and S. J. Azez, "Performance evaluation of the NACA 4415 airfoil as a model for small horizontal wind turbine blade design and operation in Iraq," 2024, p. 070029. https://doi.org/10.1063/5.0237336

[9] X. Y. Tham, C. Y. Ng, M. C. Ong, and N. F. Tingkas, "A Parametric Study on the Effect of Blade Configuration in a Double-Stage Savonius Hydrokinetic Turbine," *J. Mar. Sci. Eng.*, vol. 13, no. 5, p. 868, Apr. 2025, https://doi.org/10.3390/jmse13050868

[10] J. Park *et al.*, "CFD-based design optimization of ducted hydrokinetic turbines," *Sci. Rep.*, vol. 13, no. 1, p. 17968, Oct. 2023, https://doi.org/10.1038/s41598-023-43724-4

[11] M. I. Lamas Galdo *et al.*, "Enhanced Performance of a Hydrokinetic Turbine through a Biomimetic Design," *J. Mar. Sci. Eng.*, vol. 12, no. 8, p. 1312, Aug. 2024, https://doi.org/10.3390/jmse12081312

[12] D. A. T. D. do Rio Vaz, J. R. P. Vaz, and P. A. S. F. Silva, "An approach for the optimization of diffuser-augmented hydrokinetic blades free of cavitation," *Energy for Sustainable Development*, vol. 45, pp. 142–149, Aug. 2018, https://doi.org/10.1016/j.esd.2018.06.002

[13] M. Grabbe, K. Yuen, A. Goude, E. Lalander, and M. Leijon, "Design of an experimental setup for hydro-kinetic energy conversion," *International Journal on Hydropower and Dams*, vol. 16, no. 5, pp. 112–116, 2009, [Online]. Available: https://www.diva-portal.org/smash/get/diva2:289893/FULLTEXT02.pdf

[14] A. F. Rodriguez-Valencia, E. Escobar-Nunez, and G. A. Jaramillo-Pizarro, "Recent advances and performance characteristics of vertical axis hydrokinetic turbines: A review," *Energy Reports*, vol. 14, pp. 5170–5203, Dec. 2025, https://doi.org/10.1016/j.egyr.2025.11.080

[15] M. I. Ibrahim, M. J. Legaz, A. A. Banawan, and T. M. Ahmed, "CFD Design Optimisation for the Hydrodynamic Performance of the Novel Fin-Ring Horizontal Axis Hydrokinetic Turbine," *J. Mar. Sci. Eng.*, vol. 13, no. 2, p. 323, Feb. 2025, https://doi.org/10.3390/jmse13020323

[16] B. Knight *et al.*, "Multifidelity Cfd Analysis for Ducted Hydrokinetic Turbine Design." 2025. https://doi.org/10.2139/ssrn.5103905